Modeling and Tuning of Circular Limit Cycle Oscillator FLL With Pre-Loop Filter

Pay, M. L. & Ahmed, H.

Original citation & hyperlink:
Pay, ML & Ahmed, H 2019, 'Modeling and Tuning of Circular Limit Cycle Oscillator FLL With Pre-Loop Filter' IEEE Transactions on Industrial Electronics, vol. (In-press), pp. (In-press).
https://dx.doi.org/10.1109/TIE.2019.2892677

DOI 10.1109/TIE.2019.2892677
ISSN 0278-0046
ESSN 1557-9948

Publisher: Institute of Electrical and Electronics Engineers (IEEE)

Modeling and Tuning of Circular Limit Cycle Oscillator FLL With Pre-Loop Filter

Miao Lin Pay, Hafiz Ahmed, *Member, IEEE*

Abstract

Circular limit cycle oscillator- frequency-locked loop (CLO-FLL) is a recently proposed advanced nonlinear technique for the parameter estimation of grid voltage signal. It has fast convergence and can handle DC bias/offset. Nevertheless, the performance degrades in the presence of harmonics. In this letter, we propose the application of pre-loop filtering to enhance the robustness of CLO-FLL in the presence of harmonics. Pre-loop filtering slightly increase the computational complexity. However, number of parameters to tune remain the same. The small-signal modeling, tuning and performance comparisons of both techniques are performed in this letter.

Index Terms

Pre-loop filter, frequency estimation, phase-locked loop (PLL), frequency-locked loop (FLL)

I. Introduction

In today's distributed power system, the effect of nonlinear loads (*e.g.* adjustable speed drive, various types of power supply) can not be neglected. Nonlinear loads introduce harmonic disturbance into the grid. In addition to harmonics, DC offset may also be introduced in the grid voltage due to current transformer saturation or faults. As a result, the control system of the grid connected converters are desired to have robustness against these kind of disturbances.

Existing popular current controllers use various techniques to estimate the fundamental parameters of the grid. Applying phase-locked loop (PLL) is a popular approach in the literature [1], [2]. PLL has a trade-off between fast dynamic response and disturbance rejection capability. Moreover, performance deteriorates in the presence of harmonics and/ DC offset. To overcome the limitation of PLL, many solutions have been proposed in the literature. Enhanced PLL (EPLL) [3], adaptive notch filter (ANF) [4], second order generalized integrator - frequency-locked loop (SOGI-FLL) [5] are some of the popular ones.

EPLL consists of a frequency adaptive filter. It has been found in the literature that EPLLs dynamic response is slow and not suitable for application where fast convergence is required. SOGI-FLL and ANF both uses linear harmonic oscillator as the quadrature signal generator (QSG). Linear oscillator is not structurally stable. To overcome this limitation, nonlinear oscillators based frequency locked-loop have been proposed recently in the literature [6], [7]. Although both FLL uses limit cycle oscillator, [6] (Fig. 1a) can handle DC bias where as [7] can not. Moreover the model used in [6] is computationally simpler than [7]. As such in this work, we focus our attention to the circular limit cycle oscillator - FLL (CLO-FLL).

Although CLO-FLL has many interesting properties but it is not immune to harmonics. To make the CLO-FLL harmonic robust, one solution is to use multiple CLO filter in parallel similar to the ideas given in [5]. In this approach, one additional CLO block is needed for each harmonic frequency. This increases the computational complexity. Another solution is to use pre-filtering to extract the fundamental component. There are many types of pre-filtering methods available in the literature. In the steady-state, CLO-FLL is similar to SOGI-FLL. SOGI based pre-filtering approach has been proposed for SOGI-FLL in [8]. It has been found in [8], [9] that the presence of SOGI-based pre-loop filter in SOGI-FLL decreases

The authors are with Coventry University, The Futures Institute, Coventry CV1 2TL, United Kingdom. Corresponding author: H. Ahmed, E-mail: ac7126@coventry.ac.uk, Tel: +44-2-477650023.

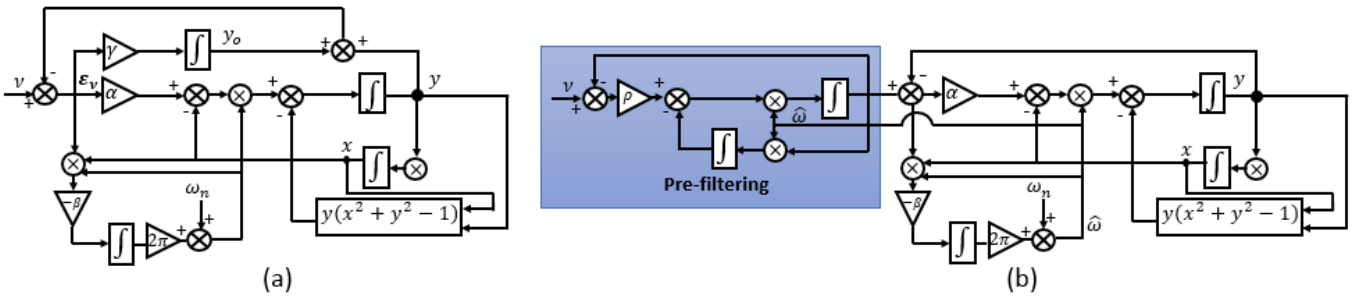

Figure 1. Block diagram of (a) CLO-FLL and (b) CLO-FLL-WPF.

the frequency estimation ripple magnitude, increases the robustness of the quadrature-phase signal to sub-harmonics, enhances the harmonic rejection property, reduces the amplitude distortion etc. Due to all these advantages, SOGI-based pre-filter is used in our work as well. CLO-FLL with pre-filter (CLO-FLL-WPF) (Fig. 1b) is the main issue of this letter. An interesting feature of CLO-FLL-WPF is that it has the same numbers of parameter to tune as that of CLO-FLL.

In this work, we first develop a linear model of the CLO-FLL which hasn't been done before in [6]. Later on, we model the CLO-FLL-WPF by extending the linear model of CLO-FLL. Based on the linear models, parameter tuning of the both technique have been done in this letter. Finally, experimental results are provided to demonstrate the effectiveness of CLO-FLL-WPF over CLO-FLL in the presence of harmonics. Modeling, tuning and performance comparison of CLO-FLL and CLO-FLL-WPF are the main contributions of this letter. The main purpose of the small-signal modeling is only to tune the gains. The results presented in this work have been motivated by [9].

II. CLO-FLL

Harmonic polluted grid voltage signal is given by

$$\nu(t) = A_0 + \sum_{i=1}^{n} A_i \sin \underbrace{(\omega_i t + \phi_i)}_{\theta_i} \tag{1}$$

where A_0 is the DC offset, A_i,ω_i,ϕ_i,$\theta_i \in [0, 2\pi)$ are the amplitude, frequency, phase and instantaneous phase of the individual frequency components respectively. To estimate the parameters of the fundamental grid voltage signal i.e. $i = 1$ in Eq. (1), in [6], CLO-FLL has been proposed. CLO-FLL can be mathematically represented as:

$$\dot{y} = \alpha(\nu - y - y_o)\hat{\omega} - x\hat{\omega} - y(x^2 + y^2 - 1) \tag{2a}$$
$$\dot{x} = y\hat{\omega} \tag{2b}$$
$$\dot{z} = -\beta(\nu - y - y_o)x\hat{\omega} \tag{2c}$$
$$\dot{y}_0 = \gamma(\nu - y - y_o) \tag{2d}$$

where $\alpha, \beta, \gamma > 0$ are the tuning gains, y is the estimate of the grid voltage signal without DC bias, y_o is the estimate of the DC bias and $\hat{\omega} = \omega_n + 2\pi z$ is the estimated grid frequency. From the x and y, the instantaneous phase and amplitude can be calculated as:

$$\hat{\theta} = \arctan(y/-x) \tag{3}$$
$$\hat{A} = \sqrt{x^2 + y^2} \tag{4}$$

In the steady-state, solution of eq. (2a) and (2b) are

$$y(t) = \hat{A}\sin(\hat{\theta}) \tag{5a}$$

$$x(t) = -\hat{A}\cos(\hat{\theta}) \tag{5b}$$

For further calculation, we assume that the grid amplitude is always normalized to unity *i.e.* measurements in per unit (p.u.) are used. Normalization is necessary for the proper functioning of the proposed technique.

A. Dynamics in the steady-state

In the steady-state *i.e.* when the oscillator converged to the circular limit cycle, the nonlinear part of the oscillator $y(x^2+y^2-1) \to 0$. In that case, substituting (1) (with $i=1$), (5a) and (5b) in eq. (2c), one can obtain the following frequency dynamics:

$$\begin{aligned}
\dot{\hat{\omega}} &= 2\pi\beta\left[A_0 + A\sin(\theta) - \hat{A}\sin(\hat{\theta}) - \hat{A}_o\right]\hat{A}\cos(\hat{\theta})\hat{\omega} \\
\dot{\hat{\omega}} &= \omega_n\beta\pi\left[\sin(\theta-\hat{\theta}) + \sin\left(\theta+\hat{\theta}\right) - \sin(2\hat{\theta})\right] \\
&\quad + \omega_n\beta\pi\left[+2(A_0-\hat{A}_0)\cos(\hat{\theta})\right] \\
\dot{\hat{\omega}} &= \omega_n\beta\pi\left\{\left(\theta-\hat{\theta}\right) + 2\left(A_0-\hat{A}_0\right)\right\}
\end{aligned} \tag{6}$$

where we assumed that $\hat{\omega} = \omega_n$, $\cos(\hat{\theta}) \approx 1, \theta \to 0$ and used the small-angle approximation formula $\sin(\theta-\hat{\theta}) \approx (\theta-\hat{\theta})$ to keep the linearity of equation (6). In the steady-state nominal case $\hat{\omega} = \omega_n$. As such this assumption is not unrealistic. In addition, we have also assumed that $\theta + \hat{\theta} \approx 2\hat{\theta}$. All these assumptions will be used in the subsequent calculations as well. From eq. (3), the dynamics of the instantaneous phase is given by:

$$\begin{aligned}
\dot{\hat{\theta}} &= \frac{-x\dot{y}+\dot{x}y}{x^2+y^2} = \frac{-x\dot{y}+\dot{x}y}{\hat{A}^2} \\
&= -x\{\alpha(\nu-y-y_o)\hat{\omega} - x\hat{\omega}\} + y^2\hat{\omega} \\
&= -\alpha x(\nu-y-y_o)\hat{\omega} + \hat{\omega}(x^2+y^2) \\
\dot{\hat{\theta}} &= (\alpha/2\pi\beta)\dot{\hat{\omega}} + \hat{\omega}
\end{aligned} \tag{7}$$

where we have used the relation $-x(\nu-y-y_o)\hat{\omega} = \dot{\omega}/2\pi\beta$ from eq. (2c). Next, the dynamics of the amplitude can be calculated from eq. (4) as:

$$\begin{aligned}
\dot{\hat{A}} &= \frac{x\dot{x}+y\dot{y}}{\sqrt{x^2+y^2}} = \frac{x\dot{x}+y\dot{y}}{\hat{A}} \\
&= \alpha y(\nu-y-y_o)\hat{\omega}/\hat{A} \\
&= \alpha\hat{\omega}\hat{A}\sin(\hat{\theta})\left[A_0 + A\sin(\theta) - \hat{A}\sin(\hat{\theta}) - \hat{A}_o\right]/\hat{A} \\
&= \frac{\alpha\omega_n}{2}\left[A\cos(\theta-\hat{\theta}) - A\cos(\theta+\hat{\theta}) + \cos(2\hat{\theta}) - \hat{A}\right] \\
&+ \alpha\omega_n\left[(A_0-\hat{A}_0)\cos(\hat{\theta})\right] \\
&= \frac{\alpha\omega_n}{2}\left[(A-\hat{A}) + 2(A_0-\hat{A}_0)\right]
\end{aligned} \tag{8}$$

Finally the dynamics of the DC bias estimation can be calculated as:

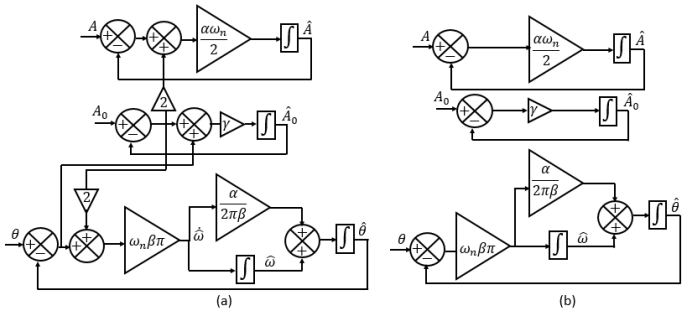

Figure 2. (a) Linearized model of CLO-FLL with cross-coupling terms, (b) Simplified linearized model without cross-coupling terms.

$$\dot{\hat{A}}_0 = \gamma\left[A_0 + A\sin(\theta) - \hat{A}\sin(\hat{\theta}) - \hat{A}_o\right]$$
$$\dot{\hat{A}}_0 = \gamma(\theta - \theta_0 + A_0 - \hat{A}_0) \tag{9}$$

where we have used the small-angle approximation formula *i.e.* $\sin(\theta) \approx \theta$ and $\sin(\hat{\theta}) \approx \hat{\theta}$.

Eq. (6), (7), (8) and (9) forms the linear model of the CLO-FLL which is given in Fig. 2 (a). In these linearized models, cross-coupling terms are present in all the equations. As such direct transfer function of individual parameters e.g. $\hat{\omega}(s)/\omega(s)$ can't be obtained. In all these equations, DC bias estimation error $i.e.\ A_0 - \hat{A}_0$ is present as the cross-coupling term. In general, the magnitude of DC bias is significantly smaller than that of the other variables. As a result, near the equilibrium point, DC bias estimation error can also be considered negligible w.r.t. other estimation errors. Linearized model in this case is given in Fig. 2 (b). From this figure, the following transfer functions can be obtained :

$$\hat{\theta}(s) = \frac{\frac{\alpha\omega_n}{2}s + \pi\omega_n\beta}{s^2 + \frac{\alpha\omega_n}{2}s + \pi\omega_n\beta}\theta(s) \tag{10a}$$
$$\hat{\omega}(s) = \frac{\pi\omega_n\beta}{s^2 + \frac{\alpha\omega_n}{2}s + \pi\omega_n\beta}\omega(s) \tag{10b}$$
$$\hat{A}(s) = \frac{\frac{\alpha\omega_n}{2}}{s + \frac{\alpha\omega_n}{2}}A(s) \tag{10c}$$
$$\hat{A}_0(s) = \frac{\gamma}{s+\gamma}A(s) \tag{10d}$$

Eq. (10) forms the basis for tuning the gain of the CLO-FLL. Since the tuning parameters of CLO-FLL are all strictly positive i.e. $\alpha, \beta, \gamma > 0$, this implies that all the denominator polynomial of Eq. (10) have positive coefficients. Second-degree polynomial with positive coefficients are Hurwitz polynomial. This ensures the stability of the linearized CLO-FLL given by Eq. (10).

B. Model based parameter tuning of CLO-FLL

The denominator of the second-order transfer functions (10a) and (10b) can be compared to the standard second-order transfer function denominator *i.e.*

$$s^2 + 2\zeta\omega_o s + \omega_o^2 = 0 \tag{11}$$

where ζ is the damping ratio and ω_o is the natural frequency. From the comparison, we find that $\zeta = \alpha\omega_n/4\omega_o$ and $\omega_o = \sqrt{\pi\omega_n\beta}$. In the control system system literature $\zeta = 1/\sqrt{2}$ has been suggested as a good value. Then the following formulas can be good starting choice for the CLO-FLL

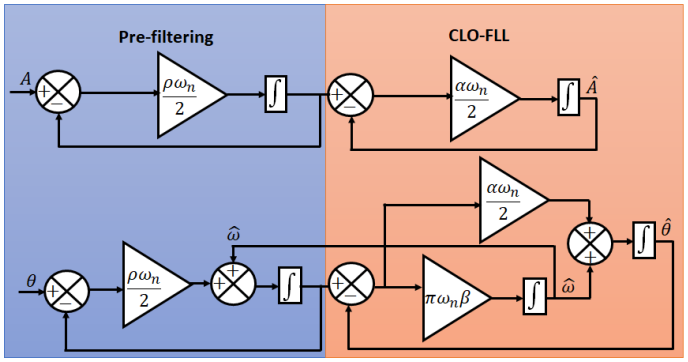

Figure 3. Linearized model of CLO-FLL-WPF.

$$\alpha = 2\sqrt{2\pi\beta/\omega_n} = 2\sqrt{\beta/f} \tag{12}$$

where experience suggests that $\beta \leq f$. Apart from α and β, there is another gain γ which determines the convergence of the DC bias estimation loop. The DC loop transfer function (10d) has the form of a standard low pass filter with unity-gain. Higher values of γ will ensure fast convergence or vice-versa. Too-high value of γ may introduce numerical instability. As such $\gamma = \sqrt{2}f$ can be considered as a good initial point. Finally CLO-FLL parameters are selected as: $\alpha = 1/\sqrt{2}$, $\beta = 6.5$ and $\gamma = 70$.

III. CLO-FLL-WPF

The block diagram of the CLO-FLL-WPF is given in Fig. 1 (b). Since pre-filtering is used for CLO-FLL-WPF, no estimation loop is required for the DC bias. Linearized model of the CLO-FLL-WPF can be obtained in the same way as described in the case of CLO-FLL. However, the calculations are very lengthy in that case. Another way is to use extend the model of CLO-FLL for the case of CLO-FLL-WPF. In this article we have considered the later approach. Linearized model of the CLO-FLL-WPF is shown in Fig. 3. From this figure, the transfer functions for CLO-FLL-WPF can be obtained as:

$$\hat{\theta}(s) = \frac{a_1 s + a_0}{s^3 + b_2 s^2 + b_1 s + b_0}\theta(s) \tag{13a}$$

$$\hat{\omega}(s) = \frac{a_0}{s^3 + b_2 s^2 + b_1 s + b_0}\omega(s) \tag{13b}$$

$$\hat{A}(s) = \frac{\frac{\alpha\omega_n}{2}\frac{\rho\omega_n}{2}}{(s + \frac{\alpha\omega_n}{2})(s + \frac{\rho\omega_n}{2})}A(s) \tag{13c}$$

where $a_1 = (\frac{\alpha\rho\omega_n^2}{4} + \frac{\alpha\omega_n^2}{2})$, $a_0 = \frac{\beta\rho\omega_n^2\pi}{2} + \pi\omega_n^2\beta$, $b_2 = (\omega_n + \frac{\alpha\omega_n}{2} + \frac{\rho\omega_n}{2})$, $b_1 = (\frac{\alpha\rho\omega_n^2}{4} + \frac{\alpha\omega_n^2}{2} + \pi\omega_n\beta)$ and $a_0 = b_0$. The above-mentioned transfer functions forms the basis for the tuning of the parameters of CLO-FLL-WPF. Similar to CLO-FLL, as all the parameters are strictly positive, denominator polynomials in Eq. (13) are Hurwitz which ensure the stability.

A. Parameter tuning for CLO-FLL-WPF

From the transfer function (13c), one can see that if $\alpha = \rho$, then the gain of the transfer function is unity which is a good value for the amplitude estimation loop. Next if we compare the denominator of the transfer function (13c) with that of eq. (11), we found that $\alpha = \rho = \sqrt{2}$ corresponds to $\zeta = 1/\sqrt{2}$.

Denominator polynomial of transfer function (13a) and (13b) are both of third order. As such they can be expressed by the following polynomial:

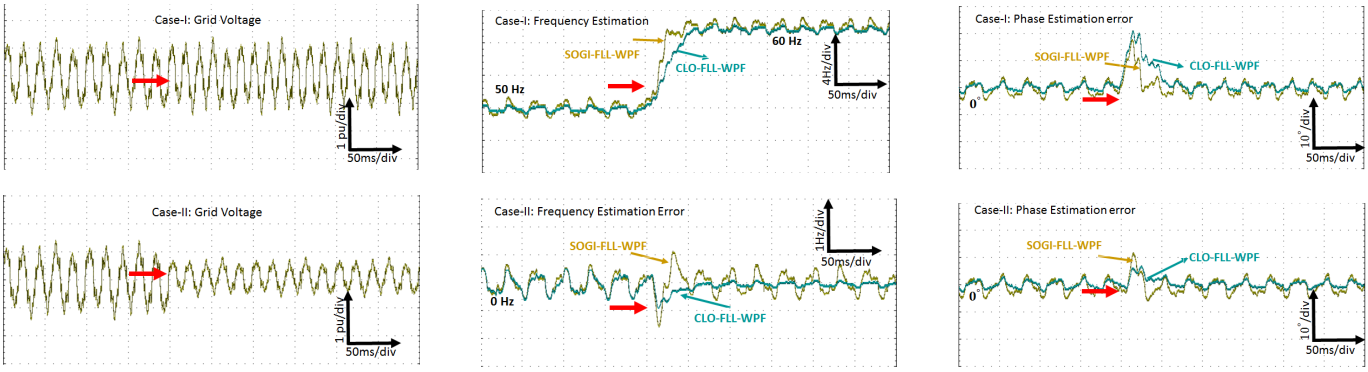

Figure 4. Comparative Experimental results for Test-I (top) and Test-II (bottom). Red arrow indicates the beginning of disturbance.

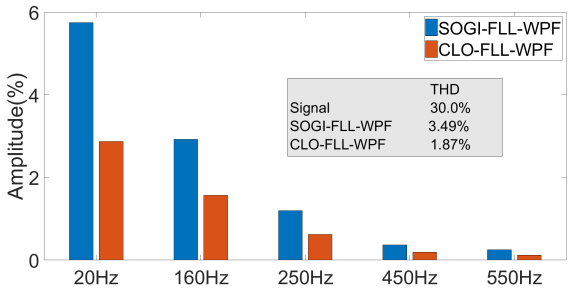

Figure 5. Harmonic distortions comparison.

$$(s+\mu\omega_0)\left(s^2+2\zeta\omega_0 s+\omega_0^2\right)=0 \tag{14}$$

where μ is the scaling factor. By comparing the coefficients of the constant term, one can obtain that $\beta=\mu\omega_n/(\pi+\pi/\sqrt{2})$. Finally CLO-FLL-WPF parameters are selected as: $\alpha=\rho=\sqrt{2}$, and $\beta=12.5$.

IV. Experimental Results

To validate the theoretical developments of the previous sections, hardware-in-the-loop (HIL) experimental studies are performed using dSPACE 1104 board with 10KHz.sampling frequency. As a comparison technique SOGI-FLL-WPF is selected with parameter values as $k_1=k_2=\sqrt{2}$ and $\lambda=23948$ [9]. The considered based signal has 30% total harmonic distortion (THD) comprised of 20Hz. sub-harmonics, 160Hz.inter-harmonics and 5^{th}, $9^{\text{th}}$and 11^{th} order harmonics with each having an amplitude of 0.15p.u. Harmonic distortions generated by both techniques are given in Fig. 5. Two experimental tests are considered.

- Test-I: Sudden frequency jump of $+10$Hz.
- Test-II: Sudden amplitude jump of -0.5p.u.

Comparative experimental results for the two cases are given in Fig. 4. Results for Test-I and II show that both technique have similar performances in terms of settling time. However, CLO-FLL-WPF has better steady state performance in terms of steady-state ripple. In addition, CLO-FLL-WPFs produced almost 50% lower THD w.r.t. SOGI-FLL-WPF. This is a clear evidence of higher harmonic filtering capability of CLO-FLL-WPF with respect to SOGI-FLL-WPF.

V. Conclusion

In this article, small-signal modeling of CLO-FLL and CLO-FLL-WPF has been carried out. Based on the linearized model, parameter tuning has been performed. With the selected gains, experimental tests

have been performed to asses the suitability of two techniques. Experimental results demonstrate that both technique have similar dynamic performance. However, CLO-FLL-WPF performs better than CLO-FLL in the presence of harmonics thanks to the pre-filtering. This comes at a cost of additional computational complexity. However, the number of gains remain the same. One issue that remain unaddressed is the concurrent optimal tuning of the CLO-FLL-WPF parameters. This issue will be considered in a future work.

REFERENCES

[1] M. Merai, W. Naouar, I. Slama-Belkhodja, and E. Monmasson, "An adaptive PI controller design for DC-link voltage control of single-phase grid-connected converters," *IEEE Transactions on Industrial Electronics*, pp. 1–1, 2018.

[2] S. Bayhan, O. Kukrer, and H. Komurcugil, "Model-based current control strategy with virtual time constant for improved dynamic response of three-phase grid-connected VSI," *IEEE Transactions on Industrial Electronics*, pp. 1–1, 2018.

[3] M. Karimi-Ghartemani, *Enhanced phase-locked loop structures for power and energy applications*. John Wiley & Sons, 2014.

[4] D. Yazdani, A. Bakhshai, G. Joos, and M. Mojiri, "A nonlinear adaptive synchronization technique for grid-connected distributed energy sources," *IEEE Transactions on Power Electronics*, vol. 23, no. 4, pp. 2181–2186, 2008.

[5] P. Rodríguez, A. Luna, I. Candela, R. Mujal, R. Teodorescu, and F. Blaabjerg, "Multiresonant frequency-locked loop for grid synchronization of power converters under distorted grid conditions," *IEEE Transactions on Industrial Electronics*, vol. 58, no. 1, pp. 127–138, 2011.

[6] H. Ahmed, S.-A. Amamra, and M. Bierhoff, "Frequency-locked loop based estimation of single-phase grid voltage parameters," *IEEE Transactions on Industrial Electronics*, 2018.

[7] E. Oviedo, N. Vazquez, and R. Femat, "Synchronization technique of grid-connected power converters based on a limit cycle oscillator," *IEEE Transactions on Industrial Electronics*, vol. 65, no. 1, pp. 709–717, 2018.

[8] J. Matas, M. Castilla, J. Miret, L. G. de Vicuña, and R. Guzman, "An adaptive prefiltering method to improve the speed/accuracy tradeoff of voltage sequence detection methods under adverse grid conditions." *IEEE Trans. Industrial Electronics*, vol. 61, no. 5, pp. 2139–2151, 2014.

[9] S. Golestan, J. M. Guerrero, J. C. Vasquez, A. M. Abusorrah, and Y. Al-Turki, "Modeling, tuning, and performance comparison of second-order-generalized-integrator-based FLLs," *IEEE Transactions on Power Electronics*, vol. 33, no. 12, pp. 10 229–10 239, Dec 2018.